

## Dynamic Nuclear Polarization with Biradicals

Kan-Nian Hu,<sup>†,‡</sup> Hsiao-hua Yu,<sup>‡</sup> Timothy M. Swager,<sup>‡</sup> and Robert G. Griffin<sup>\*,†,‡</sup>

Francis Bitter Magnet Laboratory and Department of Chemistry, Massachusetts Institute of Technology, Cambridge Massachusetts 02139

Received November 23, 2003; E-mail: rgg@mit.edu

The past few years has witnessed a renaissance in the use of dynamic nuclear polarization (DNP) to enhance signal intensities in NMR spectra of solids and liquids. In a contemporary DNP experiment, a diamagnetic sample is doped with a paramagnet and the large polarization of the electron spins is transferred to the nuclei via microwave irradiation of the EPR spectrum.<sup>1</sup> The development of gyrotron microwave sources (140 and 250 GHz)<sup>2,3</sup> has permitted these experiments to be performed at high fields (5 and 9 T), and signal enhancements ranging from 20 to 400 are observed, depending on the details of the experiments:  $B_0$ ,  $B_1$ ,  $T$ , etc.<sup>4–9</sup> The largest signal enhancements observed are in experiments where the thermal mixing (TM) or cross effect (CE) mechanisms<sup>10–14</sup> are operative. Although multiple spins may be involved in both mechanisms, the underlying physics is essentially described by a three-spin process that involves the coupling of two electrons whose frequencies,  $\omega_{e1}/2\pi$  and  $\omega_{e2}/2\pi$  in the EPR spectrum of the polarizing agent, are spaced at the nuclear Larmor frequency,  $\omega_n/2\pi$  (see Figure 1a). When these electrons are dipolar coupled, then irradiation at  $\omega_{e1}$  produces a simultaneous spin flip of the second electron at  $\omega_{e2}$  and the nucleus leading to the generation of nuclear spin polarization (Figure 1b) through transitions such as  $|\alpha_1\beta_2\beta_n\rangle \leftrightarrow |\beta_1\alpha_2\alpha_n\rangle$  or  $|\beta_1\alpha_2\beta_n\rangle \leftrightarrow |\alpha_1\beta_2\alpha_n\rangle$ . Since the introduction of the DNP technique 50 years ago,<sup>15,16</sup> all experiments have relied on monomeric paramagnetic centers such as a nitroxide or metal ion as a source of polarization. However, the  $e^-e^-$  dipole coupling is clearly an important parameter governing the efficiency of the three-spin TM and CE processes. Thus, it should be possible to optimize the enhancements in DNP experiments by constraining the distance between the two unpaired electrons. In this communication we demonstrate the validity of this concept with experiments that employ *biradical polarizing agents* consisting of two 2,2,6,6-tetramethylpiperidinyl-1-oxyl (TEMPO) radicals tethered by a poly-(ethylene glycol) chain (Figure 1c). These biradical polarizing agents yield a factor of  $\sim 4$  larger signal intensities over those obtained with monomeric TEMPO. Further, the larger enhancements are obtained at significantly lower concentrations, thereby reducing the paramagnetic broadening present in the NMR spectrum.

The biradicals illustrated in Figure 1c were prepared from 4-hydroxy-TEMPO and the di-, tri-, or tetra-ethyleneglycol-ditosylate using methods outlined by Gagnaire et al.,<sup>17</sup> yielding a series of bis-TEMPO- $n$ -ethyleneglycol (BT $n$ E) biradicals. Solution EPR spectra of BT $n$ E ( $n = 2, 3$ , or 4) (1 mM in methanol) showed the expected five lines indicating a strong exchange interaction (larger than <sup>14</sup>N hyperfine interaction) between the electrons.<sup>18</sup> Samples for the DNP experiments consisted of 5 mM biradical (10 mM electrons) and 2 M <sup>13</sup>C-urea dispersed in a 60:40 <sup>2</sup>H<sub>6</sub>-DMSO/H<sub>2</sub>O (90% <sup>2</sup>H<sub>2</sub>O) glass-forming mixture. The high concentration of <sup>13</sup>C-urea facilitated the rapid and accurate determination of the

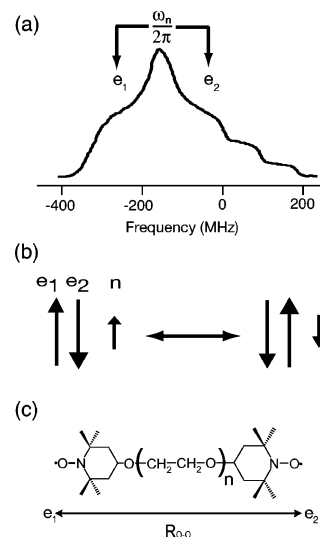


**Figure 1.** (a) Illustration of the EPR spectrum of monomeric TEMPO nitroxide. Note that the breadth of the spectrum is  $\sim 600$  MHz and is large compared to that of the <sup>1</sup>H Larmor frequency (211 MHz). The arrows indicate the approximate frequencies of the electron spins, separated by  $\omega_n/2\pi$ , expected to participate in the CE/TM DNP enhancement process (b) Illustration of the microwave-driven three-spin process associated with TM or CE DNP where two coupled electrons undergo an energy conserving flip-flop process that leads to enhanced nuclear spin polarization. (c) The molecular structure of the BT $n$ E biradicals where  $n$  is the number of ethylene glycol units that tether two nitroxide radicals (TEMPO). The dots represent the two unpaired electrons whose displacement is approximated as the oxygen–oxygen distance,  $R_{O-O}$ .

enhancement factors, but to illustrate the applicability of DNP experiments to dilute samples we include as Supporting Information a spectrum obtained from 5 mM <sup>13</sup>C-urea. A control sample of 10 mM monomeric 4-hydroxy-TEMPO was also examined. The samples were contained in 4-mm sapphire rotors, and a series of DNP/CPMAS <sup>13</sup>C spectra were recorded as a function of the microwave irradiation time using a 140-GHz gyrotron source and a low-temperature MAS probe operating at 90 K at  $\omega_p/2\pi = 3.5$  kHz.<sup>19</sup>

Figure 2 illustrates a typical nuclear polarization buildup curve obtained with a sample of BT2E. Note that the <sup>13</sup>C signal from urea is barely visible on the vertical scale used in the absence of microwave irradiation. However, with 3–15 s of microwave irradiation, the signal grows dramatically, reaching a plateau after  $\sim 15$  s where we measure an enhancement of 175. Figure 3 illustrates the dependence of the enhancement on the length of the ethylene glycol linker and shows that, as the linker is shortened from  $n = 4$  to 3 to 2 the enhancement increases from 80 to 110 and finally to 175, respectively. The estimated error is  $\pm 25$ . For 10 mM TEMPO in this solvent system we observe an enhancement of 45. Thus, tethering the two TEMPO radicals yields a factor of 3.9 larger enhancement.

<sup>†</sup> Francis Bitter Magnet Laboratory.

<sup>‡</sup> Department of Chemistry.

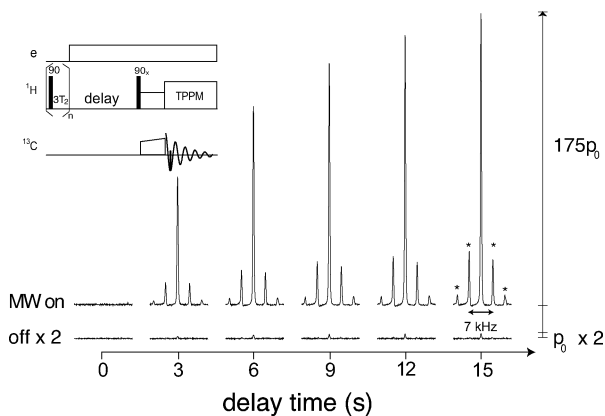


**Figure 2.**  $^{13}\text{C}$  DNP-MAS spectra illustrating the growth of the  $^{13}\text{C}$ -urea signal as the irradiation time is increased. The polarizing agent was BTZE at a concentration of 5 mM (or 10 mM electrons). As indicated in the figure, the maximum observed enhancement was  $175 \pm 25$ . The inset shows the pulse sequence used to record the spectra. It utilizes a train of saturating pulses on the  $^1\text{H}$  channel to ensure that all of the polarization arises from the DNP effect. The spectra were recorded at 90 K, using a 4-mm sapphire rotor,  $\omega_d/2\pi = 3.5$  kHz, and the microwave power was 1.5 W entering the probe.

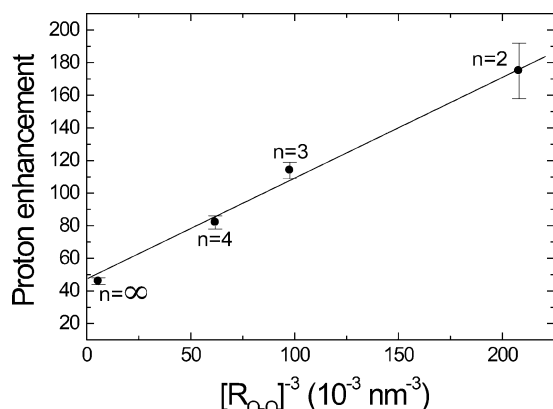


**Figure 3.** Plot of the  $^1\text{H}$  enhancement measured indirectly through the  $^{13}\text{C}$  spectrum as a function of the approximate electron–electron dipolar as measured by the distance, specifically  $[\text{R}_{\text{O-O}}]^{-3}$ . The data points show the DNP enhancements obtained from molecules corresponding to the monomeric TEMPO ( $n = \infty$ ) and the three biradicals that are tethered with 4, 3, and 2 poly(ethylene glycol) units. Notice that the shorter the linker the larger the enhancement. The electron concentration in all of the samples was 10 mM corresponding to a concentration of 5 mM for the biradical molecules and 10 mM for monomeric TEMPO. The enhancements were recorded at 90 K at  $\omega_d/2\pi = 3.5$  kHz.

As can be surmised from Figure 1, the efficiency of the CE DNP process is affected by the polarizing agent through the size of the  $e^-e^-$  dipole coupling and the relative orientations of the two radicals. At present we have not measured either of these quantities experimentally. However, an estimate of the  $e^-e^-$  dipole coupling can be made using the intraradical distance obtained from a simulated conformation assuming an all-trans polymer chain.<sup>20</sup> The value of  $\text{R}_{\text{O-O}}$  from such specific conformations leads to approximate dipole couplings of 3.3, 5.2, and 11.0 MHz for the three BTnE ( $n = 4, 3,$  and  $2$ ) compounds, respectively. Further, the simulations suggest that the TEMPOs at either end of the linker are oriented so that the planes of their rings are approximately  $90^\circ$  with respect to one another. Thus, when the magnetic field is perpendicular to the ethylene glycol chain, the molecular orientation of the  $g$ -tensors<sup>21,22</sup> leads to a frequency difference between the two TEMPO molecules approximately equal to  $\omega_n/2\pi$  that would support the CE.

To achieve a larger DNP enhancement we could naively extrapolate the approximate linear dependence illustrated in Figure 3 to a  $(\text{R}_{\text{O-O}})^{-3}$  value corresponding to a shorter linker. The shortest biradical in BTnE series is BT1n and with an estimated  $\text{R}_{\text{O-O}}$  of 1.43 nm ( $\omega_d/2\pi = 18.5$  MHz) which could yield a DNP enhancement of  $\sim 250$ . Achieving this value may depend on the  $e^-e^-$  dipole coupling ( $\omega_d$ ) remaining small compared to the frequency separation illustrated in Figure 1 and the CE mechanism dominating the DNP. In contrast, when the dipole coupling is strong—i.e. when  $|\omega_d| \approx |\omega_n|$ —the two coupled electrons form a ground-state triplet,<sup>18,23</sup> and in this case the TM DNP mechanism contributes to the polarization process. Thus, synthesis of biradicals with a variety of different rigid linkers containing two TEMPO radicals and radicals that are different from TEMPO are in progress. These new polarizing agents together with studies of the high-field EPR spectrum and the measurement of DNP enhancements will help us to distinguish between situations where CE or TM is the dominant enhancement mechanism. These experiments are in progress and will be reported in future publications.

**Acknowledgment.** This research was supported by the National Institutes of Health through Grants EB002804 and EB002026. We acknowledge stimulating conversations with our colleagues V. Bajaj, D. Ingu, C.-G. Joo, M. Hornstein, R. J. Temkin, and M. Veshtort, and the invaluable technical assistance of J. Bryant. In addition, we have discussed the idea of biradical polarizing agents with several former colleagues whom we acknowledge: G. Gerfen, L. Becerra, D. Hall, S. Inati, V. Weis, M. Bennati, and M. Rosay.

**Supporting Information Available:** A DNP-enhanced  $^{13}\text{C}$  MAS spectrum of a 5 mM solution of  $^{13}\text{C}$ -urea, illustrating that the experiments described herein are applicable to solute concentrations in the millimolar regime. This material is available free of charge via the Internet at <http://pubs.acs.org>.

## References

- Wind, R. A. *Prog. Nucl. Magn. Reson. Spectrosc.* **1985**, *17*, 33–67.
- Becerra, L. R.; Gerfen, G. J.; Bellew, B. F.; Bryant, J. A.; Hall, D. A.; Inati, S. J.; Weber, R. T.; Un, S.; Prisner, T. F.; McDermott, A. E.; Fishbein, K. W.; Kreischer, K. E.; Temkin, R. J.; Singel, D. J.; Griffin, R. G. *J. Magn. Reson. A* **1995**, *117*, 28–40.
- Kreischer, K. E.; Farrar, C. T.; Griffin, R. G.; Temkin, R. J.; Viereg, J. *Proc. 24th Int. Conf. Infrared and Millimeter Waves* **1999**, IU-A3.
- Becerra, L. R.; Gerfen, G. J.; Temkin, R. J.; Singel, D. J.; Griffin, R. G. *Phys. Rev. Lett.* **1993**, *71*, 3561–3564.
- Gerfen, G. J.; Becerra, L. R.; Hall, D. A.; Griffin, R. G.; Temkin, R. J.; Singel, D. J. *J. Chem. Phys.* **1995**, *102*, 9494–9497.
- Weis, V.; Bennati, M.; Rosay, M.; Bryant, J. A.; Griffin, R. G. *J. Magn. Reson.* **1999**, *140*, 293–299.
- Rosay, M.; Zeri, A. C.; Astrof, N. S.; Opella, S. J.; Herzfeld, J.; Griffin, R. G. *J. Am. Chem. Soc.* **2001**, *123*, 1010–1011.
- Rosay, M.; Weis, V.; Kreischer, K. E.; Temkin, R. J.; Griffin, R. G. *J. Am. Chem. Soc.* **2002**, *124*, 3214–3215.
- Bajaj, V. S.; Farrar, C. T.; Hornstein, M. K.; Mastovsky, I.; Viereg, J.; Bryant, J.; Elena, B.; Kreischer, K. E.; Temkin, R. J.; Griffin, R. G. *J. Magn. Reson.* **2003**, *160*, 85–90.
- Kessenikh, A. V.; Manenkov, A. A. *Sov. Phys. Solid State (Engl. Transl.)* **1963**, *5*, 835–837.
- Hwang, C. F.; Hill, D. A. *Phys. Rev. Lett.* **1967**, *18*, 110–112.
- Hwang, C. F.; Hill, D. A. *Phys. Rev. Lett.* **1967**, *19*, 1011–1013.
- Wollan, D. S. *Phys. Rev. B* **1976**, *13*, 3671–3685.
- Wollan, D. S. *Phys. Rev. B* **1976**, *13*, 3686–3696.
- Overhauser, A. W. *Phys. Rev.* **1953**, *92*, 411–415.
- Carver, T. R.; Slichter, C. P. *Phys. Rev.* **1953**, *92*, 212–213.
- Gagnaire, G.; Jeunet, A.; Pierre, J. L. *Tetrahedron Lett.* **1991**, *32*, 2021–2024.
- Luckhurst, G. In *Spin Labeling: Theory and Applications*; Berliner, L. J., Ed.; Academic Press: New York, 1976; pp 133–181.
- Rosay, M.; Lansing, J. C.; Haddad, K. C.; Bachovchin, W. W.; Herzfeld, J.; Temkin, R. J.; Griffin, R. G. *J. Am. Chem. Soc.* **2003**, *125*, 13626–13627.
- Pfannebecker, V.; Klos, H.; Hubrich, M.; Volkmer, T.; Heuer, A.; Wiesner, U.; Spiess, H. W. *J. Phys. Chem.* **1996**, *100*, 13428–13432.
- Griffith, O. H.; Cornell, D. W.; McConnell, H. M. *J. Chem. Phys.* **1965**, *43*, 2909–2910.
- Libertini, L. J.; Griffiths, O. H. *J. Chem. Phys.* **1970**, *53*, 1359–1367.
- Norris, J. R.; Weissman, S. I. *J. Phys. Chem.* **1969**, *73*, 3119–3124.

JA039749A